

The background of the slide is a photograph of a modern glass skyscraper, likely a TU Delft building, viewed from a low angle looking up. The building's facade is composed of a grid of windows and structural elements. A dark blue vertical bar is visible on the far left edge of the slide.

Algebraic flux correction schemes for B-spline based finite elements

Delft Institute of Applied Mathematics
Numerical Analysis Group

Matthias Möller (m.moller@tudelft.nl)

May 21, 2015

The TU Delft logo is located in the bottom left corner. It features a stylized flame or bird-like icon above the letters 'TU Delft'. The 'TU' is in a bold, dark blue font, and 'Delft' is in a dark grey font.

TU Delft

Outline

1 Motivation

2 Mathematical building blocks

Introduction to isogeometric analysis

Principles of Algebraic Flux Correction

3 Applications

Constrained data projection

Constrained transport

Human brain development

4 Outlook

Vision

Unified simulation and design optimization toolkit

Multi-physics simulation

- complex coupled processes
- different models and scales
- different discretizations
- different resolutions

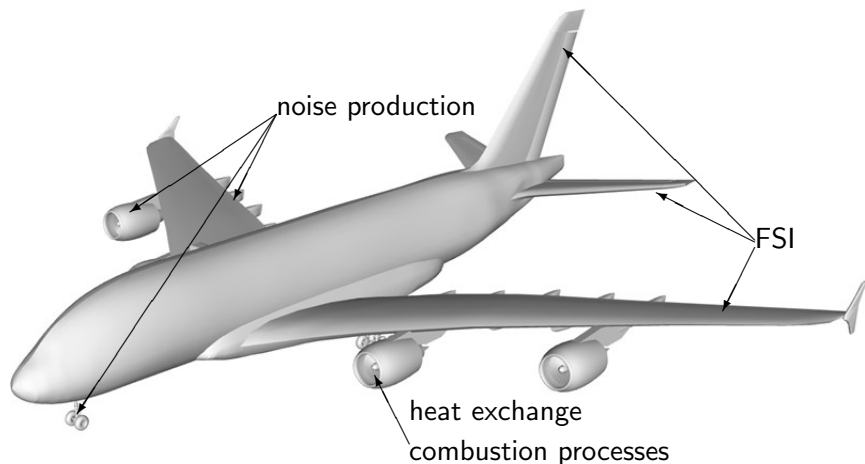
Multi-objective optimization

- (mutually excluding) goals
- adjoint based-optimization
- derivative-free methods
- hierarchical optimization

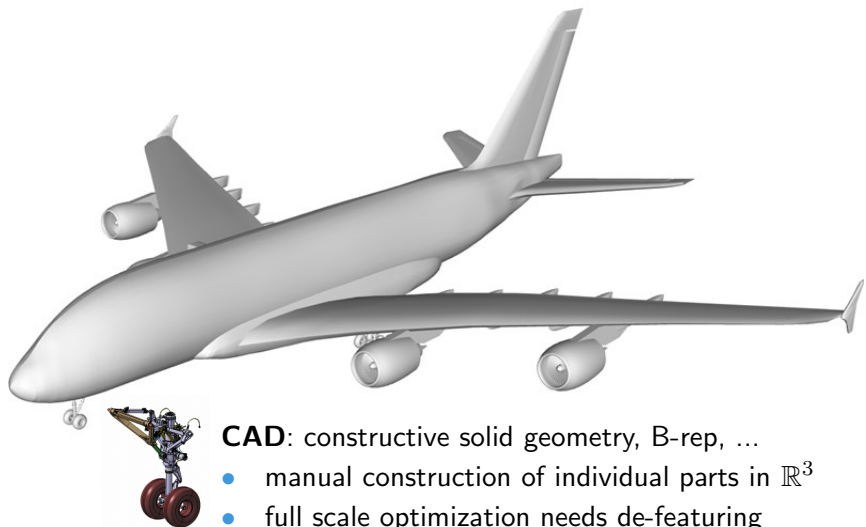
Commonalities

- **one common multi-component master geometry**
- amount of data requires parallel/distributed computing
- problem complexity requires HPC programming techniques

Multiple problems, one master geometry



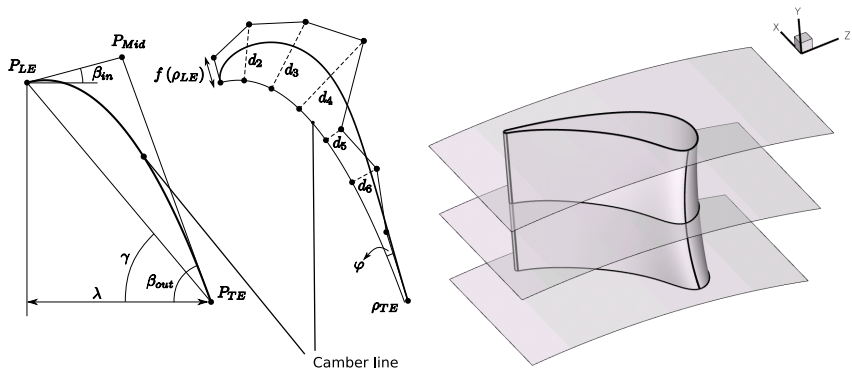
Multiple problems, one master geometry



CAD: constructive solid geometry, B-rep, ...

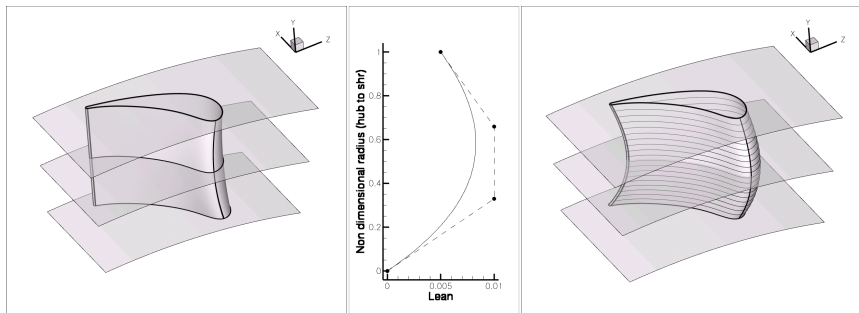
- manual construction of individual parts in \mathbb{R}^3
- full scale optimization needs de-featuring

Axial turbine blade geometry generation¹



¹T. Verstraete. "CADO: a Computer Aided Design and Optimization Tool for Turbomachinery Applications". In: *Proc. of the 2nd International Conference on Engineering Optimization*. 2010.

Axial turbine blade geometry generation¹



- direct control of parameters in k -dimensional design space
- moderate number of design parameters in optimization procedure

¹T. Verstraete. "CADO: a Computer Aided Design and Optimization Tool for Turbomachinery Applications". In: *Proc. of the 2nd International Conference on Engineering Optimization*. 2010.

Isogeometric Analysis

The solution to all our problems?

Vision of the inventors²: **Full CAD-CAE integration**

- 1 Create *analysis-suitable* geometry in CAD tool (using NURBS, B-splines, T-splines, hierarchical splines, ...)
- 2 Apply established FEA-tools using the same spline basis functions as test and trial functions in the variational form
- 3 Perform automatic design optimization on the control points of the CAD geometry or, at best, in the design parameter space

²T.J.R. Hughes, J.A. Cottrell, and Y. Bazilevs. “Isogeometric Analysis: CAD, finite elements, NURBS, exact geometry and mesh refinement”. In: *Computer Methods in Applied Mechanics and Engineering* 194 (2005), pp. 4135–4195.

Isogeometric Analysis

A practical solution to some problems.

After 10 years of practical experience ...

- solid theoretical basis has been established
- succesfull application in fluid and solid mechanics, FSI, ...
- early-adoption in open-source and commercial codes (LSDYNA)

However, ...

- (manual) post-processing of CAD geometries is still required
- assembly of system matrices is more costly than in standard FEA
- global higher continuity in multi-patch scenario is challenging
- very little research pursued on efficient solution techniques
- even less research pursued on IgA for compressible flows

Isogeometric Analysis

A promising concept with large research potential!

IgA for convection-dominated and compressible flows

- algebraic stabilization methods based on matrix manipulations
- efficient assembly based on Fletcher's group formulation
- positivity-preserving time-stepping methods, e.g., SSP-RK

Efficient solution techniques

- outer discontinuous Galerkin multi-patch approach
- multi-level iterative solution algorithms

Heterogeneous HPC

- optimized single-patch compute-kernels for different platforms
- exploit compute-intensity and tensor-product construction of IgA

Outline

1 Motivation

2 Mathematical building blocks

Introduction to isogeometric analysis

Principles of Algebraic Flux Correction

3 Applications

Constrained data projection

Constrained transport

Human brain development

4 Outlook

Spline space $\mathcal{S}(\Omega_0, p, \mathcal{M}, \mathcal{P})$

- **Polynomial space** of degree p over interval $\Omega_0 := [a, b] \subset \mathbb{R}$

$$\Pi^p([a, b]) := \{q(x) \in C^\infty([a, b]) : q(x) = \sum_{i=0}^p c_i x^i, c_i \in \mathbb{R}\}$$

- **Polynomial spline** of degree p defined as $s : \Omega_0 \mapsto \mathbb{R}$ if

$$s|_{[x_i, x_{i+1}]} \in \Pi^p([x_i, x_{i+1}]), \quad i = 1, \dots, k$$
$$\frac{d^j}{dx^j} s_{j-1}(x_i) = \frac{d^j}{dx^j} s_i(x_i), \quad i = 2, \dots, k, j = 0, \dots, p - m_i$$

for partition $\mathcal{P} := \{a = x_1 < \dots < x_{p+1} = b\}$ of the interval Ω_0
and a set of positive integers $\mathcal{M} := \{1 \leq m_i \leq p + 1\}$

B-splines

- **Knot vector** is sequence of non-decreasing coordinates $\xi_i \in [a, b] \subset \mathbb{R}$ in the parameter space $\Omega_0 = [a, b]$

$$\Xi = (\xi_1, \xi_2, \dots, \xi_{n+p+1}), \quad \text{where}$$

- $\xi_i \in \mathbb{R}$ is the i^{th} knot with knot index i
 - p is the polynomial order of the B-splines
 - n is the number of B-spline functions
- **Open knot vector** for $(\Omega_0, p, \mathcal{P}, \mathcal{M})$ is defined as

$$\Xi = \left(\underbrace{a, \dots, a}_{p+1 \text{ times}}, \dots, \underbrace{x_i, \dots, x_i}_{m_i \text{ times}}, \dots, \xi_n, \underbrace{b, \dots, b}_{p+1 \text{ times}} \right)$$

B-splines, cont'd

- **B-splines** of order p yield a basis of the spline space

$$\mathcal{S}(\Omega_0, p, \mathcal{M}, \mathcal{P}) = \mathcal{S}(\Xi, p) := \text{span}\{N_{i,p}(\xi), i = 1, \dots, n\}$$

- **Cox-de Boor recursion formula**

$$p = 0 : N_{i,0}(\xi) = \begin{cases} 1 & \text{if } \xi_i \leq \xi < \xi_{i+1} \\ 0 & \text{otherwise} \end{cases}$$

$$p > 0 : N_{i,p}(\xi) = \frac{\xi - \xi_i}{\xi_{i+p} - \xi_i} N_{i,p-1}(\xi) + \frac{\xi_{i+p+1} - \xi}{\xi_{i+p+1} - \xi_{i+1}} N_{i+1,p-1}(\xi)$$

with „ $\frac{0}{0}$ “ := 0“

B-splines, cont'd

- **Derivative** of B-spline of order p is a B-spline of order $p - 1$

$$\frac{d}{d\xi} N_{i,p}(\xi) = \frac{p}{\xi_{i+p} - \xi_i} N_{i,p-1}(\xi) - \frac{p}{\xi_{i+p+1} - \xi_{i+1}} N_{i+1,p-1}(\xi)$$

- Expression for k^{th} **derivative** of B-spline of order p

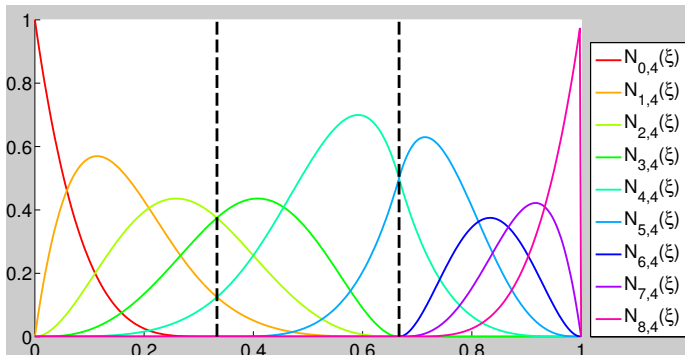
$$\frac{d^k}{d^k \xi} N_{i,p}(\xi) = \frac{p!}{(p-k)!} \sum_{j=0}^k \alpha_{k,j} N_{i+j,p-k}(\xi)$$

with recursively defined coefficients $\alpha_{k,j}$ ³

³L. Piegl and W. Tiller. *The NURBS book*. Second edition. Springer, 1997.

Nonuniform continuity at element boundaries

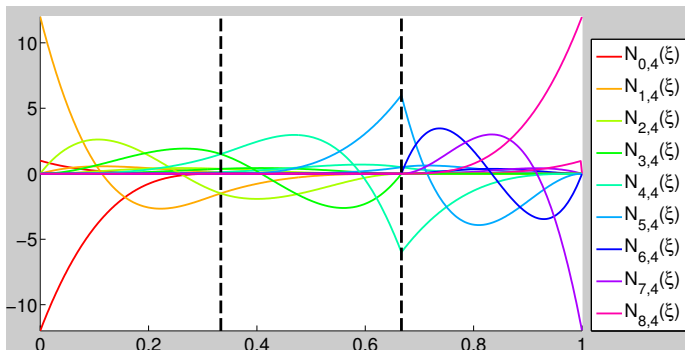
4th-order B-spline functions



$$\Xi = \underbrace{(0, 0, 0, 0, 0)}_{\text{discontinuity}}, \underbrace{1/3}_{C^3}, \underbrace{2/3, 2/3, 2/3}_{C^1}, \underbrace{1, 1, 1, 1, 1}_{\text{discontinuity}}$$

Nonuniform continuity at element boundaries

First derivatives of 4th-order B-spline functions



$$\Xi = \left(\underbrace{0, 0, 0, 0, 0}_{\text{discontinuity}}, \underbrace{1/3}_{C^3}, \underbrace{2/3, 2/3, 2/3}_{C^1}, \underbrace{1, 1, 1, 1, 1}_{\text{discontinuity}} \right)$$

Properties of B-splines

- B-splines form a **partition of unity**

$$\text{For each } \xi \in [a, b] : \sum_{i=1}^n N_{i,p}(\xi) = 1 \quad \Rightarrow \quad \sum_{i=1}^n N'_{i,p}(\xi) = 0$$

- B-splines of order p have **compact support**

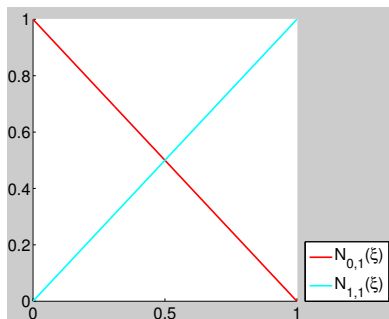
$$\text{supp } N_{i,p}(\xi) = [\xi_i, \xi_{i+p+1}), \quad i = 1, \dots, n$$

- B-splines are **strictly positive** over the interior of their support

$$N_{i,p}(\xi) > 0 \quad \text{for } \xi \in (\xi_i, \xi_{i+p+1}), \quad i = 1, \dots, n$$

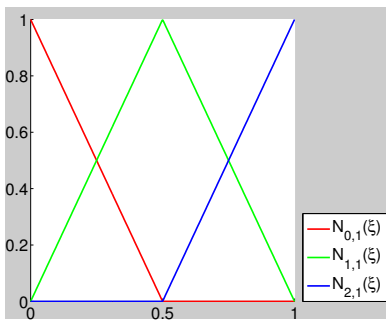
Knot insertion

$$\Xi = (0, 0, 1, 1), p = 1$$



one element

$$\Xi = (0, 0, 0.5, 1, 1), p = 1$$

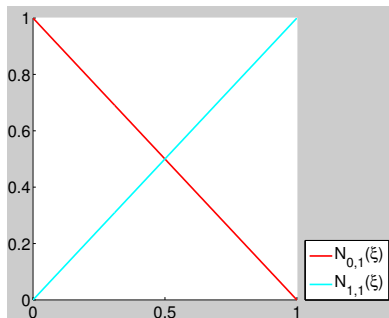


two elements, C^0 -continuity

Equivalent to classical h -refinement for knot insertion with $m_{\text{new}} = p$

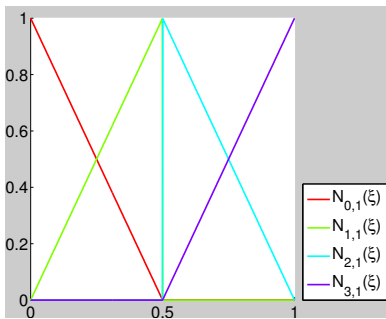
Knot insertion, cont'd

$$\Xi = (0, 0, 1, 1), p = 1$$



one element

$$\Xi = (0, 0, 0.5, 0.5, 1, 1), p = 1$$

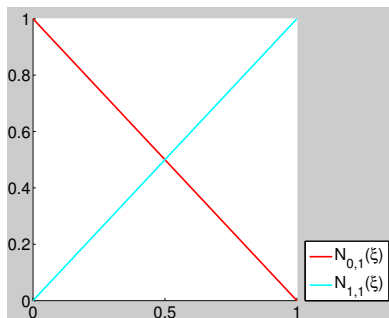


two elements, discontinuity

Enables continuity reduction(!) for knot insertion with $m_{\text{new}} > p$

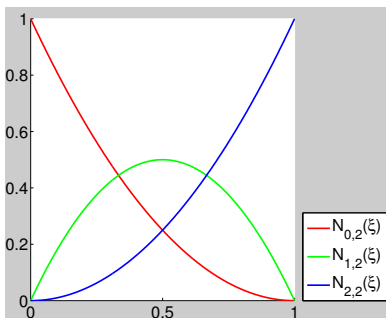
Order elevation

$$\Xi = (0, 0, 1, 1), p = 1$$



one element

$$\Xi = (0, 0, 0, 1, 1, 1), p = 2$$



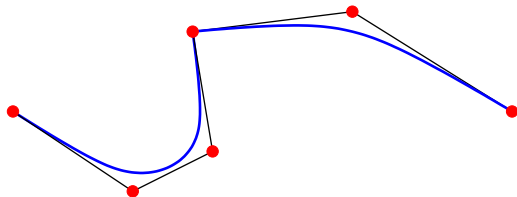
one element

No negative values as with Lagrange basis functions for $p \geq 2$

B-spline curves

- **B-spline curves:** geometric mapping $\mathbf{G} : \Omega_0 \mapsto \Omega$

$$\mathbf{G}(\xi) = \sum_{i=1}^n N_{i,p}(\xi) \mathbf{p}_i \quad \text{with control points } \mathbf{p}_i \in \mathbb{R}^d, d \geq 1$$



- **B-spline surfaces:** geometric mapping $\mathbf{G} : \Omega_0 \mapsto \Omega$

$$\mathbf{G}(\xi) = \sum_{i=1}^n N_{i,p}(\xi) \mathbf{p}_i \quad \text{with control points } \mathbf{p}_i \in \mathbb{R}^d, d \geq 1$$

B-spline surfaces

- Multi-variate B-spline basis for $\Omega_0 = [a, b] \times [c, d]$

$$\mathcal{S}(\Xi, \mathcal{H}, p, q) = \text{span}\{N_{i,p}(\xi)N_{j,q}(\eta), i = 1..n, j = 1..m\}$$

- Geometric mapping $\mathbf{G} : \Omega_0 \mapsto \Omega$

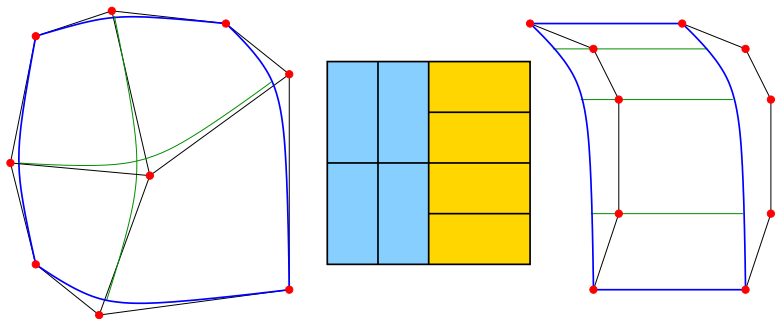
$$\mathbf{G}(\xi, \eta) = \sum_{i=1}^n \sum_{j=1}^m N_{i,p}(\xi)N_{j,q}(\eta)\mathbf{p}_{ij}, \quad \mathbf{p}_{ij} \in \mathbb{R}^d, d \geq 2$$

- Global basis functions (e.g., line-wise numbering)

$$N_a(\xi, \eta) = N_{i,p}(\xi)N_{j,q}(\eta), \quad a = n(j - 1) + i$$

- Canonical generalization to higher dimensions including partition of unity, local support and strict positivity property

Multi-patch B-spline surfaces



- Possibility for different p/q and n/m -values per patch
- Use, e.g., Z-ordering for improved locality of DoFs
- Consider only single-patch domains in this talk

Ansatz spaces

- Construct ansatz space from B-spline basis functions

$$V_h = \text{span}\{\varphi_a(\mathbf{x}) = N_a \circ \mathbf{G}^{-1}(\mathbf{x}), \mathbf{x} \in \Omega\}$$

- Approximate the solution the standard way

$$u(\mathbf{x}, t) \approx u_h = \sum_{a=1}^N \varphi_a(\mathbf{x}) u_a(t)$$

- Approximate fluxes by Fletcher's group formulation

$$f(u(\mathbf{x}, t)) \approx f_h = \sum_{a=1}^N \varphi_a(\mathbf{x}) f_a(t), \quad f_a(t) = f(u_a)$$

Principles of Algebraic Flux Correction

- **Discrete diffusion operators**⁴ are symmetric $N \times N$ matrices with zero row and column sums

$$D = \{d_{ab}\}, \quad d_{ab} = d_{ba}, \quad d_{aa} := -\sum_{b \neq a} d_{ab}$$

- Decomposition into edge-contributions

$$[Du]_a = \sum_b d_{ab} u_b = d_{aa} u_a + \sum_{b \neq a} d_{ab} u_b = \sum_{b \neq a} f_{ab}$$

$$[Du]_b = \sum_{a \neq b} f_{ba}, \quad f_{ba} = -f_{ab}, \quad f_{ab} = d_{ab}(u_b - u_a)$$

⁴KT2002.

Row-sum mass lumping

- Consistent mass matrix

$$M = \{m_{ab}\}, \quad m_{ab} = \int_{\Omega} \varphi_a(\mathbf{x})\varphi_b(\mathbf{x})d\mathbf{x}$$

- Row-sum lumped mass matrix

$$M_l := \text{diag}(m_a), \quad m_a = \sum_b m_{ab}$$

- Discrete mass diffusion operator

$$D = M - M_l, \quad d_{ab} = m_{ab}, \quad d_{aa} := - \sum_{b \neq a} m_{ab}$$

Principles of Algebraic Flux Correction, cont'd

- Generic discrete system (strong imposition of bc's)

$$\begin{bmatrix} A_{\Omega} & A_{\Gamma} \\ 0 & I \end{bmatrix} \begin{bmatrix} u_{\Omega} \\ u_{\Gamma} \end{bmatrix} = \begin{bmatrix} B_{\Omega} & B_{\Gamma} \\ 0 & I \end{bmatrix} \begin{bmatrix} g_{\Omega} \\ g_{\Gamma} \end{bmatrix}$$

with matrix coefficients

$$a_{aa} > 0, \forall a \quad a_{ab} \leq 0, \forall a, b \neq a \quad b_{ab} \geq 0, \forall a, b \quad (1)$$

- Local **discrete maximum principle** (proof⁵)

$$(\text{??}) \wedge \sum_b a_{ab} = \sum_b b_{ab} \quad \Rightarrow \quad u_a^{\min} \leq u_a \leq u_a^{\max}$$

⁵K2012a.

Principles of Algebraic Flux Correction, cont'd

- Generic discrete system as before with matrix coefficients

$$a_{aa} > 0, \forall a \quad a_{ab} \leq 0, \forall a, b \neq a \quad b_{ab} \geq 0, \forall a, b \quad (2)$$

and strictly or irreducibly diagonally dominant matrix A . (3)

Then A is an **M-Matrix**, i.e. $A^{-1} \geq 0$.

- Global **discrete maximum principle** (proofs⁶)

$$(\text{??}) \wedge (3) \wedge \sum_b a_{ab} = \sum_b b_{ab}, \forall a \quad \Rightarrow \quad \min g \leq u \leq \max g$$

⁶K2012a.

Outline

1 Motivation

2 Mathematical building blocks

Introduction to isogeometric analysis

Principles of Algebraic Flux Correction

3 Applications

Constrained data projection

Constrained transport

Human brain development

4 Outlook

Constrained data projection⁷

- **High-order predictor:** consistent L_2 -projections

$$\sum_b m_{ab} u_b^H = \int_{\Omega} \varphi_a f \, d\mathbf{x}$$

- **Low-order predictor:** lumped L_2 -projections

$$m_a u_a^L = \int_{\Omega} \varphi_a f \, d\mathbf{x}$$

- Prelimited raw antidiffusive flux ($f_{ba} = -f_{ab}$)

$$f_{ab} = \begin{cases} m_{ab}(u_a^H - u_b^H), & \text{if } (u_a^H - u_b^H)(u_a^L - u_b^L) > 0 \\ 0, & \text{otherwise} \end{cases}$$

⁷D. Kuzmin et al. "Failsafe flux limiting and constrained data projections for equations of gas dynamics". In: *Journal of Computational Physics* 229.23 (2010), pp. 8766–8779. ISSN: 0021-9991. DOI: <http://dx.doi.org/10.1016/j.jcp.2010.08.009>. URL: <http://www.sciencedirect.com/science/article/pii/S0021999110004468>.

Constrained data projection, cont'd

- Bounds and antidiffusive increments

$$Q_a^\pm = \max_{b \neq a} \min(0, u_a^L - u_b^L), \quad P_a^\pm = \sum_{b \neq a} \max_{\min}(0, f_{ab})$$

- Nodal and edge-wise limiting coefficients

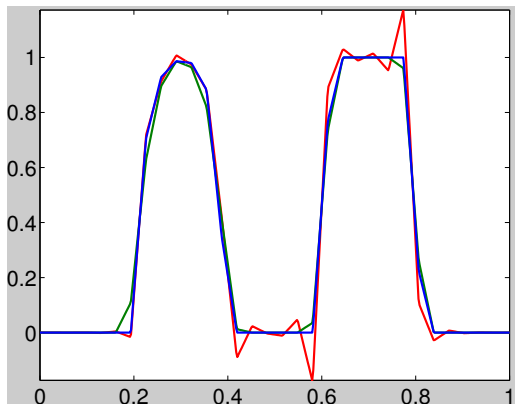
$$R_a^\pm = \frac{m_a Q_a^\pm}{P_a^\pm}, \quad \alpha_{ab} = \begin{cases} \min(R_a^+, R_b^-), & \text{if } f_{ab} > 0 \\ \min(R_b^+, R_a^-), & \text{if } f_{ab} < 0 \end{cases}$$

- **Corrector:** constrained L_2 -projection

$$u_a^* = u_a^L + \frac{1}{m_a} \sum_{b \neq a} \alpha_{ab} f_{ab}, \quad 0 \leq \alpha_{ab} = \alpha_{ba} \leq 1$$

Test case: Semi-ellipse of McDonald

$p = 1, n = 32$



L_1 -/ L_2 -errors

$$\|u^H - u\|_1 = 0.0653$$

$$\|u^L - u\|_1 = 0.0684$$

$$\|u^* - u\|_1 = 0.0606$$

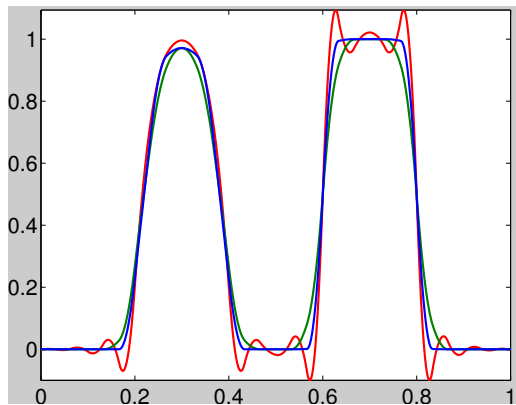
$$\|u^H - u\|_2 = 0.1774$$

$$\|u^L - u\|_2 = 0.1686$$

$$\|u^* - u\|_2 = 0.1677$$

Test case: semi-ellipse of McDonald

$p = 2, n = 32$



L_1 -/ L_2 -errors

$$\|u^H - u\|_1 = 0.0351$$

$$\|u^L - u\|_1 = 0.0568$$

$$\|u^* - u\|_1 = 0.0352$$

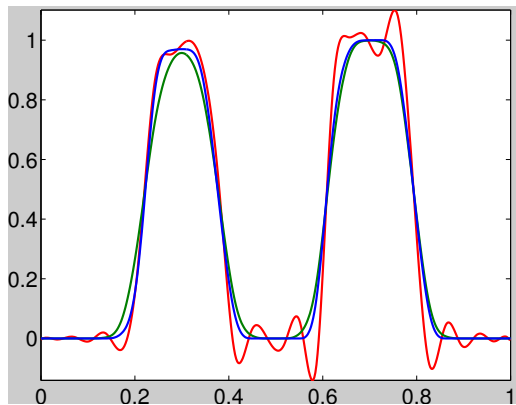
$$\|u^H - u\|_2 = 0.0748$$

$$\|u^L - u\|_2 = 0.1121$$

$$\|u^* - u\|_2 = 0.0892$$

Test case: semi-ellipse of McDonald

$p = 3, n = 32$



L_1 -/ L_2 -errors

$$\|u^H - u\|_1 = 0.0595$$

$$\|u^L - u\|_1 = 0.0788$$

$$\|u^* - u\|_1 = 0.0615$$

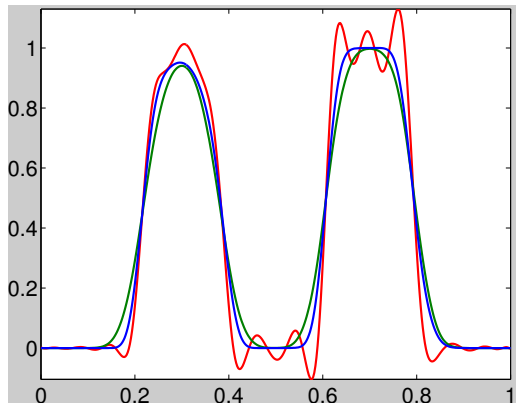
$$\|u^H - u\|_2 = 0.1213$$

$$\|u^L - u\|_2 = 0.1435$$

$$\|u^* - u\|_2 = 0.1317$$

Test case: semi-ellipse of McDonald

$p = 4, n = 32$



L_1 -/ L_2 -errors

$$\|u^H - u\|_1 = 0.0480$$

$$\|u^L - u\|_1 = 0.0896$$

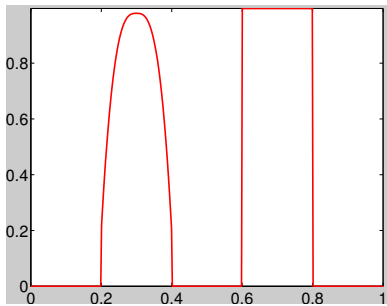
$$\|u^* - u\|_1 = 0.0608$$

$$\|u^H - u\|_2 = 0.1014$$

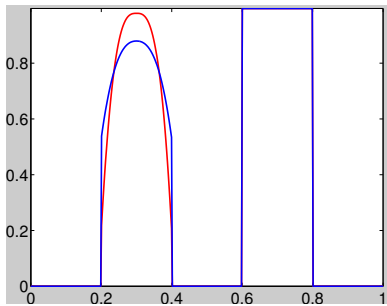
$$\|u^L - u\|_2 = 0.1505$$

$$\|u^* - u\|_2 = 0.1252$$

Thought experiment: What are ideal knots?



Thought experiment: What are ideal knots?



L_1 -/ L_2 -errors

$$\|u^H - u\|_1 = 0.0037$$

$$\|u^* - u\|_1 = 0.0220$$

$$\|u^H - u\|_2 = 0.0091$$

$$\|u^* - u\|_2 = 0.0615$$

- Deduce ideal knots from nodal correction factors or residual
 $\Xi = (0, 0, 0, 0, 0.1, 0.2, 0.2, 0.2, 0.2, 0.3, 0.4, 0.4, 0.4, 0.4, 0.5,$
 $0.6, 0.6, 0.6, 0.6, 0.7, 0.7, 0.7, 0.8, 0.8, 0.8, 0.8, 0.9, 1, 1, 1, 1)$
- Smoothness indicator is used to avoid peak clipping.

Constrained transport

- Stationary convection-diffusion equation

$$\begin{aligned}\nabla \cdot (\mathbf{v}u) - d\Delta u &= 0 && \text{in } \Omega \\ u &= g && \text{on } \Gamma_D \\ \nabla u \cdot \mathbf{n} &= 0 && \text{on } \Gamma_N\end{aligned}$$

- **High-order Galerkin scheme:** $(K + S)u^H = 0$

$$K = \{\mathbf{v}_b \cdot \int_{\Omega} \varphi_a \nabla \varphi_b \, d\mathbf{x}\}, \quad S = \{d \int_{\Omega} \nabla \varphi_a \cdot \nabla \varphi_b \, d\mathbf{x}\}$$

- **Low-order scheme:** $(K + D + S)u^L = 0$

$$D = \{d_{ab}\}, \quad d_{ab} := -\max\{k_{ab}, 0, k_{ba}\}$$

Constrained transport, cont'd

- **High-resolution scheme:** $(K + D + S)u^* + \text{lim}(-Du) = 0$
- Raw antidiffusive flux $f_{ab} = d_{ab}(u_b - u_a) = -f_{ba}$
- Bounds and antidiffusive increments

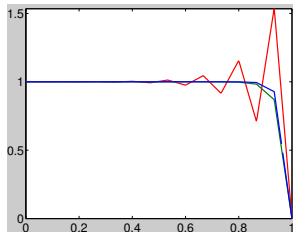
$$Q_{a/b}^{\pm} = \sum_{b \neq a} \max_{\min} (0, -/+ f_{ab}), \quad P_a^{\pm} = \sum_{b \neq a} \max_{\min} (0, f_{ab})$$

- Nodal and edge-wise limiting coefficients

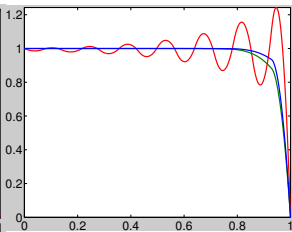
$$R_a^{\pm} = \min\left\{1, \frac{Q_a^{\pm}}{P_a^{\pm}}\right\}, \quad \alpha_{ab} = \begin{cases} R_a^+, & \text{if } f_{ab} > 0 \\ R_a^-, & \text{if } f_{ab} < 0 \end{cases}$$

Test case: convection-diffusion $\frac{v}{d} = 100$

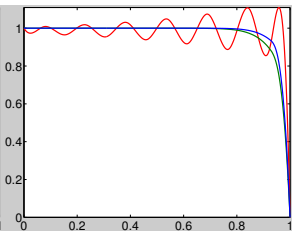
$p = 1, n = 16$



$p = 2, n = 16$



$p = 3, n = 16$



$$\|u^H - u\|_1 = 0.0325$$

$$\|u^H - u\|_1 = 0.0415$$

$$\|u^H - u\|_1 = 0.0365$$

$$\|u^L - u\|_1 = 0.0056$$

$$\|u^L - u\|_1 = 0.0061$$

$$\|u^L - u\|_1 = 0.0059$$

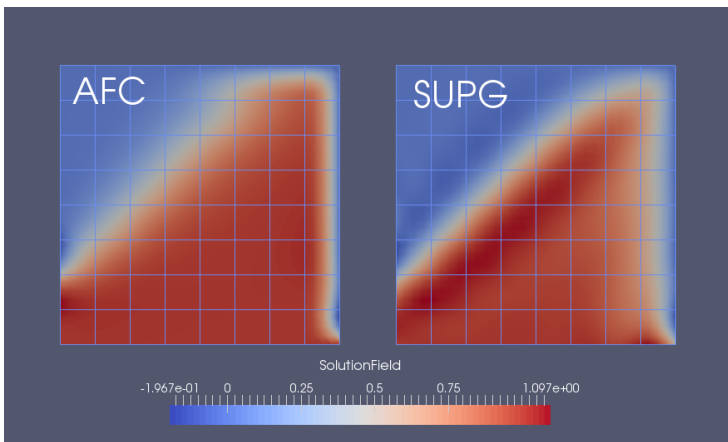
$$\|u^* - u\|_1 = 0.0028$$

$$\|u^* - u\|_1 = 0.0031$$

$$\|u^* - u\|_1 = 0.0029$$

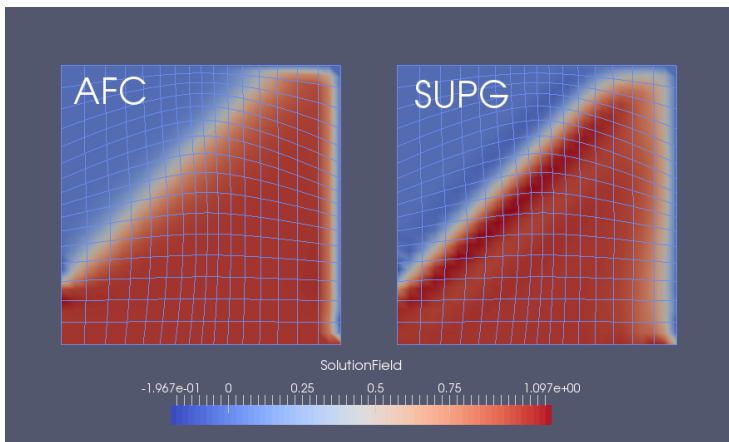
Test case: convection-diffusion

- Configuration: $\Omega = (0, 1)^2$, $d = 0.001$, $\mathbf{v} = \frac{1}{\sqrt{2}}(1, 1)^\top$
- MSc-project by Andrzej Jaeschke using G⁺SMO (JKU, Linz)



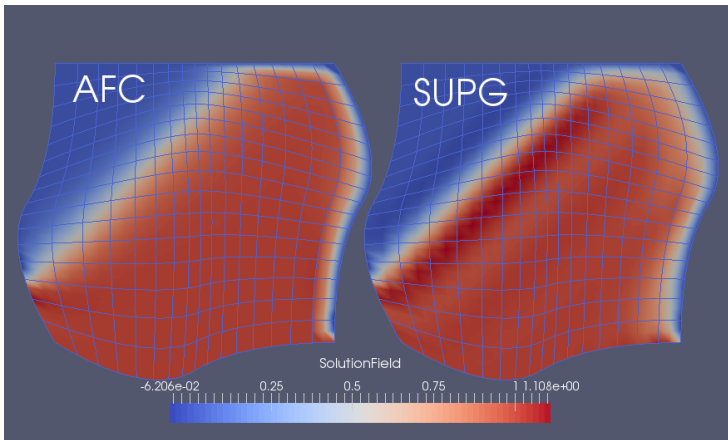
Test case: convection-diffusion

- Configuration: $\Omega = (0, 1)^2$, $d = 0.001$, $\mathbf{v} = \frac{1}{\sqrt{2}}(1, 1)^\top$
- MSc-project by Andrzej Jaeschke using G⁺SMO (JKU, Linz)



Test case: convection-diffusion

- Configuration: $\Omega = (0, 1)^2$, $d = 0.001$, $\mathbf{v} = \frac{1}{\sqrt{2}}(1, 1)^\top$
- MSc-project by Andrzej Jaeschke using ~~G~~**G⁺SMO** (JKU, Linz)



Human brain development⁸

- Gray-Scott reaction-diffusion model

$$\partial_t u + u \partial_t \log \sqrt{g_t} - d_1 \Delta_{\mathcal{M}_t} u = f(1 - u) - uv^2 \quad (\text{inhibitor } u)$$

$$\partial_t v + v \partial_t \log \sqrt{g_t} - d_2 \Delta_{\mathcal{M}_t} v = uv^2 - (f + k)v \quad (\text{activator } v)$$

with determinant $\sqrt{g_t}$ of the surface parameterization

- Surface evolution model (morphogen-driven evolution)

$$\partial_t \mathcal{M} = h(u, v) \mathbf{n}, \quad \text{e.g., } h(u, v) = Kv$$

- MSc-project by Jochen Hinz using Nutils (TU/e)

⁸J. Lefèvre and J.-F. Mangin. “A Reaction-Diffusion Model of Human Brain Development”. In: *PLoS Computational Biology* 6.4 (2009).

Summary

- Algebraic flux correction concept has been generalized to higher-order approximations based on B-spline bases
- Original lowest-order approximation is naturally included
- Nodal correction factors/residual provide information to locally reduce 'inter-element' continuity by increasing knot multiplicity
- Peak clipping at smooth extrema is prevented by locally deactivating the flux limiter using the smoothness indicator⁹

⁹D. Kuzmin and F. Schieweck. "A parameter-free smoothness indicator for high-resolution finite element schemes". In: *Central European Journal of Mathematics* 11.8 (2013), pp. 1478–1488.

Current and future research

- Theoretical analysis of AFC principles for
 - arbitrary geometric mappings, NURBS basis functions, and
 - weakly imposed boundary conditions/multi-patch coupling
- Realization of more schemes of the AFC-type family
 - transport with highly anisotropic diffusion
- Implementation of an HPC IgA-framework in C++-11
 - exploit compute-intensity of high-order methods
 - accelerator support via expression templates for assembly
 - on-demand target-optimized compilation at run time

Acknowledgements: B. Jüttler (JKU, Linz), A. Mantzaflaris (RICAM, Linz), G. v. Zwieten (TU/e, Eindhoven), and A. Jaeschke & J. Hinz & J. v. Zwieten (TUD, Delft)